Thermal ion orbit loss and radial electric field in DIII-D

J.S. deGrassie¹, J.A. Boedo², B.A. Grierson³

¹General Atomics, P.O. Box 85608, San Diego, California, 92186-5608 USA

²University of California San Diego, La Jolla, California, 92093, USA

³Princeton Plasma Physics Laboratory, Princeton New Jersey 08543, USA

email of first author: degrassie@fusion.gat.com

A relatively simple model for the generation of the radial electric field, $E_{\rm r}$, near the

outboard boundary in a tokamak is presented. The model posits that $E_{\rm r}$ is established to

supply the return current necessary to balance the thermal ion orbit loss current.

Comparison with DIII-D data is promising. Features of the model that promote a more

negative edge $E_{\rm r}$ are higher ion temperature, lower density, lower impurity ion content, and

a shorter pathlength for orbit loss. These scalings are consistent with experimentally

established access to the high-confinement mode edge transport barrier.

PACS Nos.: 52.55.Fa, 52.20.Dq, and 52.25.Fi

Shear in the radial electric field, $E_{\rm r}$, is believed to be responsible for the reduction of turbulent transport and the concomitant edge H-mode transport barrier in the tokamak [1]. Here we examine thermal ion orbit loss as a means of generating a sheared edge $E_{\rm r}$. We do not address the bifurcation that triggers a barrier.

A relatively simple neoclassical (NC) model for $E_{\rm r}$ near the outboard last closed flux surface (LCFS) in DIII-D is presented [2]. $E_{\rm r}$ is determined by balancing the return current with the thermal ion orbit loss current. This model has been motivated by recent Mach probe measurements of an edge co- I_p bulk ion flow layer in this region [3-5], with the velocity profile typically in qualitative agreement with a simple thermal ion orbit empty loss-cone model [6,7]. Simulations [8-10] have revealed a steady state particle distribution function (pdf) in this spatial region having a depleted loss cone [9,10]. The probe measurements have also shown that there can be a relatively large positive radial electric field, $E_{\rm r} \sim 10$ kV/m, just inside the LCFS in Ohmic conditions in DIII-D [5]. These two emerging indications, an empty loss-cone edge pdf from simulations and a significant probe-measured positive $E_{\rm r}$ in Ohmic discharges have motivated the development of this return current model.

Here, we postulate that the return current can be provided by the confined thermal ions near the edge, and in particular that a collisional neoclassical mechanism is sufficient. In full-f, guiding center, Monte Carlo XGC0 simulations of the H-mode pedestal region, Battaglia et al have concluded that NC physics is largely adequate to describe the ions in this region [9]. Our approach is to see if a simplified collisional return current model predicts the measured value of E_r very near the outboard edge of the plasma, and we find reasonable agreement, although as will be shown, the error bars are relatively large. The

non-Maxwellian nature of the orbit loss pdf means that self collisions drive the pdf toward a Maxwellian, and the resultant particle transport in velocity space generates charge transport in real space given the finite drift orbit widths.

Of course, in steady state there is no time averaged radial current. In developing a simple thermal ion orbit loss cone model [6,7] the steady state "return current" for the ion loss was postulated to be anomalous electron loss, leaving the lost ion mechanical momentum to provide an edge flux. The mechanism of balancing ion orbit loss with anomalous electron loss has been considered by several who seek closure to a steady state solution by incorporating theoretical models of the turbulence that provides the anomalous electron loss [11,12]. Here, we use a return current due to thermal ions. The momentum balance would involve a viscous stress, as discussed for biased electrode current injection [13], but with a non-Maxwellian pdf.

A collisional ion return current has been addressed by Shaing [14] where it is also pointed out that E_r adjusts to provide the return current. The steady state pdf is required, and here we use the approximation that this pdf is given by a Maxwellian with an empty loss cone.

First, we consider a single ion species. The NC return current results from the $E_{\rm r}/B_{\theta}$ precessing trapped ions undergoing friction with passing ions, where B_{θ} is the poloidal magnetic field strength. The empty loss cone pdf is utilized, a Maxwellian with a hole [6,7], and all the boundary regions in velocity space for trapped, passing, and lost ions are taken to depend upon the local $E_{\rm r}$ [7]. The loss cone depends upon the plasma shape also, notably the major radius of the X-point [6]. The empty loss cone pdf results in a co- $I_{\rm p}$ bulk ion velocity, $U_{\rm co}$ peaking near the outboard LCFS and decaying going inward on the scale

of the poloidal ion gyroradius, $\rho_{\theta} = \overline{v}/\omega_{\theta}$, with $\overline{v} = \sqrt{T_{i}/M_{i}}$ and $\omega_{\theta} = Z_{i}eB_{\theta}/M_{i}$ [6,7]. The friction from the portion of U_{co} carried by confined co-passing ions can drive a return current even if $E_{r} = 0$. For relatively high collisionality conditions (i.e. low T_{i}) E_{r} may even be positive with sufficient return current driven by $U_{co} - E_{r}/B_{\theta}$ to balance the loss current, possibly explaining the positive E_{r} probe measurements in the edge of some Ohmic discharges in DIII-D.

For the loss current we consider only a region within roughly one $ho_{\scriptscriptstyle{ heta}}$ of the LCFS, where we make the approximation that the loss cone in velocity space is the relatively simple region defined by all pitch angles that allow counter- I_p starting ions to reach the X-point of a single null diverted discharge [6,7]. This velocity space boundary depends upon E_r , and with $E_r \neq 0$ becomes dependent on the particle kinetic energy, $M_i v^2 / 2$ [7]. The velocity space sink computation is made tractable by assuming the width of the boundary layer pdf at the loss pitch angle, p_x , is given by diffusion in pitch angle taken over a parallel streaming time, $\tau_{\parallel} = L_{\parallel} / |\mathbf{v}_{\parallel}| = L_{\parallel} / |\mathbf{v}| |\mathbf{v}_{\parallel}| = L_{\parallel} / |\mathbf{v}| |\mathbf{v}_{\parallel}|$, with L_{\parallel} the path length from starting point to the X-point loss. This $\sqrt{\left\langle \Delta \xi^2 \right\rangle} = \sqrt{2 D_{\xi\xi} \tau_{\parallel}} = \sqrt{\upsilon_{\rm d} \left(1 - \xi^2\right) \tau_{\parallel}} \;, \quad {\rm with} \quad \upsilon_{\rm d} \quad {\rm the \quad ion-ion \quad deflection \quad frequency \quad and \quad } \\$ $\xi = \cos(p)$ taken at $p = p_x(v, E_r)$. Performing the integrations over a Maxwellian pdf outside the loss cone in velocity space we obtain, for a single ion species, $j_{\text{loss}} = Z_i e n_i \rho_\theta v_d \tilde{\lambda} I_{\text{loss}}$ for the local loss current, with I_{loss} a dimensionless number of order unity and $\tilde{\lambda} = (\overline{v}/v_d L_{\parallel})^{1/2} = (\text{mfp}/L_{\parallel})^{1/2}$, where mfp = the mean free path for pitch angle is $j_{ret} = -Z_i e n_i \rho_{\theta} v_d f_{co} f_{tr} (\tilde{U}_{co} + \Delta)$, scattering. The with return current

 $\Delta = -E_{\rm r}/(B_{\theta}\overline{\rm v}) = R\partial\Phi/\partial\Psi/\overline{\rm v}$, with $\Phi = \Phi(\Psi)$ the electric potential assumed constant on a poloidal-flux surface, , $\tilde{\rm U}_{\rm co} = {\rm U}_{\rm co}^*/\overline{\rm v}$, with ${\rm U}_{\rm co}^*$ the portion of ${\rm U}_{\rm co}$ carried by co-passing ions, and $f_{\rm co}$ and $f_{\rm tr}$ the fraction of co-passing and trapped ions; $f_{\rm co}$, $f_{\rm tr}$, $\tilde{\rm U}_{\rm co}$, and $I_{\rm loss}$ are functions of Δ . In the integrations we have approximated $v_{\rm d} = v_{\rm d}(\overline{\rm v})$, while retaining the v dependence of the other integrand terms. We note that our $j_{\rm loss}$ agrees reasonably well with Shaing's kinetic theory calculation [14] with $\tilde{\lambda} \to 1/\sqrt{v}^*$ and Δ and ρ_{θ} used to construct an effective squeezing factor for comparison. There also can be a trapped electron contribution to $j_{\rm ret}$, but for typical DIII-D edge conditions this is negligible. Equating $j_{\rm ret} + j_{\rm loss} = 0$ leads to

$$\tilde{\lambda} = f_{co} f_{tr} (\tilde{U}_{co} + \Delta) / I_{loss}$$
 (1)

where all terms on the RHS are functions of Δ , that is, $E_{\rm r}$, and $\tilde{\lambda}$ is determined experimentally by measurements of $T_{\rm i}$ and densities at the orbit starting location, with $L_{\rm ll}$ taken from the EFIT-computed equilibrium [15].

The scaling in equation (1) agrees with some general experimental observations. On the RHS the strongest variation with Δ comes from the linear term where Δ appears explicitly. The LHS varies as $\tilde{\lambda} \sim T_{\rm i} / \sqrt{n_{\rm i} L_{\parallel}}$. Isolating the explicit Δ term, we have $E_{\rm r} \sim a - b T_{\rm i} / \sqrt{n_{\rm i} L_{\parallel}}$ where a and b vary relatively weakly with $E_{\rm r}$. We see that increasing $T_{\rm i}$ makes $E_{\rm r}$ more negative. Turning this around, to obtain more negative $E_{\rm r}$ the ion temperature must be increased [16]. If a sufficiently negative $E_{\rm r}$ is a necessary condition for an H-mode transition, as implied experimentally [1], then the plasma must be heated sufficiently. Along this same reasoning, raising the density will require higher $T_{\rm i}$, that is, more ion heating power [11]. Lastly, larger L_{\parallel} also requires more heating power. This is consistent

with an increased power threshold for the X-point placed opposite the $\vec{B}x\vec{\nabla}B$ drift direction [17]. Including the NC polarization current in the current balance provides the equation for the temporal evolution of E_r , $\varepsilon_{\rm NC}\partial E_r/\partial t=-(j_{\rm ret}+j_{\rm loss})$, where $\varepsilon_{\rm NC}=n_{\rm i}M_{\rm i}/B_\theta^2$ is the NC dielectric [18]. Steady state is established on the collisional timescale and we will apply this limit to obtain equation (1). This limit neglects any time lag between $j_{\rm ret}$ and $j_{\rm loss}$, which could lead to oscillation in E_r in the temporal equation at low enough collisionality.

We neglect any turbulent particle transport which is potentially largely ambipolar in the edge. Also neglected is any interaction with neutrals such as charge exchange, which does not modify the local charge density, or collisions. We would consider both to add an effect of greater collisionality.

In order to compare with DIII-D experimental results we need to include the dominant impurity species, carbon. Even relatively small amounts of fully stripped carbon make a significant difference in the value of $E_{\rm r}$ at a given $\tilde{\lambda}$. We consider the return current to be carried by both ${\rm C^{6+}}$ and the main ion, typically ${\rm D^{+}}$ for DIII-D. For species i, the return current is

$$j_{\text{ret,i}} = -\sum_{k} Z_{i} e n_{i} \rho_{\theta i} v_{ik} f_{cok} f_{ti} (U_{co_{-k}} / \overline{v}_{i} - \Delta_{i})$$
(2)

where the k summation is over ion species. The scale length of the thermal ion loss current for each species is $\rho_{\theta k}$. For C^{6+} this is $1/\sqrt{6}$ smaller compared with D^+ at the same T_i . We focus upon a location ~ 1 $\rho_{\theta_- D^+}$ inside the LCFS and set the thermal carbon loss, and also $U_{co_-C^{6+}}$ to 0 at this location. The D^+ loss current is increased by collisions with carbon. Using $j_{\rm ret} + j_{\rm loss} = 0$ we arrive at the multi-species version of equation (1), with four terms on the RHS from equation (2).

$$\tilde{\lambda}_{1} = \left\{ A_{Z_{-}I} f_{t_{-}I} \left[D + B_{I_{-}C} (1 - f_{t_{-}C}) \Delta_{I} \right] + A_{Z_{-}C} f_{t_{-}C} \left[B_{C_{-}I} D + B_{C_{-}C} (1 - f_{t_{-}C}) \Delta_{I} \right] \right\} / I_{loss}^{Zeff}$$
(3)

where $D = f_{\text{trap_I}} \left(\tilde{U}_{\text{co_I}} + \Delta_{\text{I}} \right)$, and subscript I refers to the main ion, the A's and B's are functions of Z_{I} , Z_{eff} , and M_{I} , the main ion mass number. These are defined such that $\tilde{\lambda}_{\text{I}}$ is defined with no carbon present, $Z_{\text{eff}} = Z_{\text{I}}$, that is, we parameterize the ratio $n_{\text{C}} / n_{\text{D}}$ by Z_{eff} and define the terms in (3) such that Z_{eff} is contained only on the RHS.

Time traces from a low NBI power discharge in DIII-D are shown in Fig. 1. The X-point of this single null shape is in the $\vec{B}x\vec{\nabla}B$ drift direction. This discharge is dominated by intrinsic rotation conditions in that minimal NBI torque is injected. The large NBI "blips" in Fig. 1(a) are used for the CER [19] measurements of C^{6+} ion density, temperature and velocity, from which ion radial force balance is used to compute E_r . These blips contain both co- I_p and counter- I_p directed NBI to eliminate a net toroidal impulse. The first such blip triggers a brief H-mode transition, noted by "H" in Fig. 1(b). Then at t=2000 ms electron cyclotron heating (ECH) is added, Fig. 1(b), and another H-mode transition follows, and low power steady NBI power is added. In this phase the ECH and NBI powers are approximately 0.6 MW and 0.5 MW, respectively. As the discharge evolves through these phases the edge ion temperature rises.

In Fig. 2 we plot the measured $E_{\rm r}$, as variable Δ , versus $T_{\rm i}$, the ion temperature, over the time range shown in Fig. 1, demonstrating that $E_{\rm r}$ does become more negative as $T_{\rm i}$ rises, as the scaling seen in equation (1). The spatial location is at $\tilde{\psi}$ = 0.98 about 8 mm inside of the LCFS which is $\sim \rho_{\theta_{-}{\rm D}^{+}}$. Here, $\tilde{\psi}$ is the normalized poloidal flux minor radius coordinate.

For detailed comparison we select the timeslice at t = 2088ms, indicated by the vertical line in Fig. (1), and the larger circle (orange online) in Fig. (2). At this time the kinetic measurements at $\tilde{\psi} = 0.98$ and the equilibrium are used in the solution of equation (3). We solve for the family of solutions of $\tilde{\lambda}_1$ as a function of Δ and $Z_{\rm eff}$ over a relevant range of variation in these parameters. The solution contours are shown in Fig. (3) by $\tilde{\lambda}_1$ - computed . First, note that the addition of carbon makes Δ more negative, that is, $E_{\rm r}$ more positive. At constant density and temperature $\tilde{\lambda}_{_1}$ is constant. Following a $\tilde{\lambda}_{_1}$ - $_{\text{computed}}$ contour as Z_{eff} is increased we trace out this decrease of positive Δ in Fig. (3). The rate of decrease with increasing $Z_{\rm eff}$ is greater for the smaller $\tilde{\lambda}_{\rm l}$ -computed contours, that is, for smaller $T_{\rm i}$. The sensitivity of the model to the measurements is also indicated in Fig. 3. The straight lines indicate the measured Δ and $Z_{\mbox{\scriptsize eff}}$ from CER, the shaded region show the error bars. For these conditions a value of Δ =0.4 corresponds to $E_{\rm r} \simeq$ -13 kV/m. The model prediction for these conditions is $\tilde{\lambda}_1$ - computed = 1.8 as shown by the contour intersected. The contour of the measured value, $\tilde{\lambda}_1$ - measured = 1.3, is also shown, measured to $\sim \pm 10\%$ (error band not shown) using L_{\parallel} =20 m from the equilibrium. Within the error bar limits in Fig. 3 there is a significant variation of the computed $\tilde{\lambda}_{_{\! 1}}$, approximately +/- 1/3, indicating the challenge for detailed experimental verification. Nevertheless, the level of agreement of this simple model with all of the approximations used validates an effort to increase the accuracy of the model in the future.

A phenomenological circuit for the generation of $E_{\rm r}$ in this model is shown in Fig. 4 to illustrate the various effects in the steady-state limit having $|j_{\rm ret}| = |j_{\rm loss}|$. For a given loss

current $E_{\rm r}$ is determined by the "emf" from $U_{\rm co}$ and we define an "orthogonal conductivity", σ_{\perp} [20]. Even with $E_{\rm r}=0$ there is a drive for the return current from $U_{\rm co}$. In experiments with significant auxiliary heating other species can contribute to the two legs of the circuit, i.e. fast ions in NBI or ICRF heated plasmas, which could affect the circuit through $j_{\rm loss}$, or the emf term if the fast ion distribution has a net toroidal velocity in the edge region. A related circuit model is shown as Fig 1 in [13] considering $E_{\rm r}$ generation in biased electrode experiments. There, a voltage source is applied whereas we consider orbit loss to be a current source (or sink).

The ion radial force balance equation must of course be satisfied. In the interior, sources of particles, energy and momentum coupled with transport determine the kinetic profiles. Then, some neoclassical or turbulence effect determines thermal ion poloidal velocity and force balance is used to determine $E_{\rm r}$. However, in the very edge with a dominant sink, radial current balance may determine $E_{\rm r}$ and it is probable then that the least constrained quantity would be the poloidal velocity [21].

A spatially local balance of loss and return current density at the outboard midplane is used. At low collisionality all confined orbits pass through this location. Adding orbit loss just inside the LCFS removes some counter-Ip orbits from this region and co-Ip orbits from the inside midplane, the latter having a higher energy threshold for loss [6]. Some fraction of the surface area would enter a computation of the currents and we have tacitly taken equal areas for the loss and return current.

Model locality also means that no radial gradients are included, so there are no local Pfirsch-Schlüter or diamagnetic flows considered. These effects could be added by

including a weighting of the confined pdf that depends on ξ . Rather, we are focusing upon the effect of the loss-cone non-Maxwellian pdf.

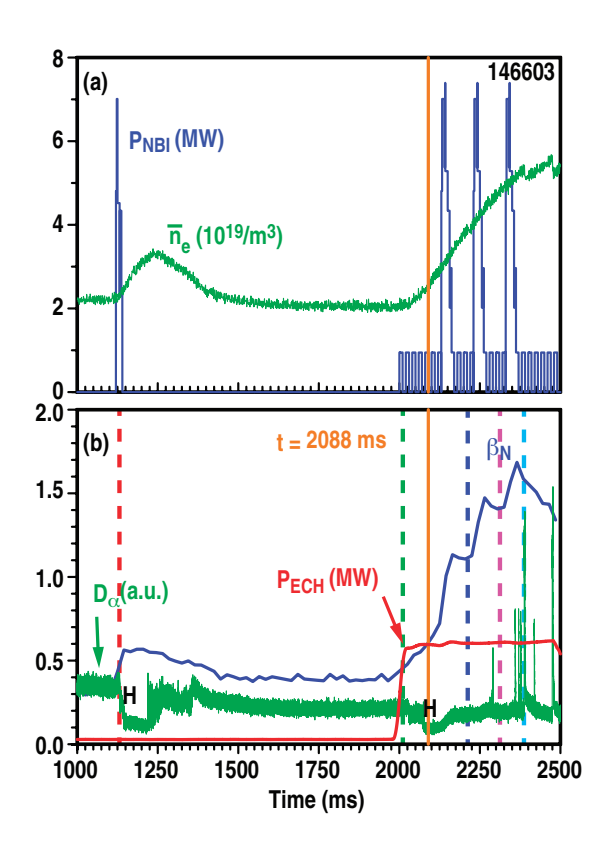
The evolution of the return current with heating, with increasing T_i , leading to increasingly negative E_r may be important for the L-H transition bifurcation, in the least for the heating phase leading up to the bifurcation. Measurements have shown that the shear in E_r , dE_r/dr , precedes an increase in the (negative) edge pressure gradient [1]. The natural localization of this neoclassical return current, due to the localization of the thermal loss current, provides an increasingly larger E_r shear with heating. The model indication of higher T_i for higher Z_{eff} or L_{\parallel} is also borne out by experiment, the latter related to the X-point location versus the $\vec{B}x\vec{\nabla}B$ drift direction [17].

This material is based upon work supported by the U.S. Department of Energy, Office of Science, Office of Fusion Energy Sciences, using the DIII-D National Fusion Facility, a DOE Office of Science user facility, under Awards DE-FC02-04ER54698, DE-FG02-95ER54309, DE-FG02-07AER54917, and DE-AC02-09CH11466. DIII-D data shown in this paper can be obtained in digital format by following the links at https://fusion.gat.com/global/D3D_DMP

- [1] R.A. Moyer, K.H. Burrell, T.N. Carlstrom, S. Coda, R.W. Conn, E.J. Doyle, P. Gohil, R.J. Groebner, J. Kim, R. Lehmer, W.A. Peebles, M. Porkolab, C.L. Rettig, T.L. Rhodes, R.P. Seraydarian, R. Stockdale, D.M. Thomas, G.R. Tynan and J.G. Watkins, Phys. Plasmas 2, 2397 (1995).
- [2] J.S. deGrassie, J.A. Boedo, B.A. Grierson and R.J. Groebner, "Thermal ion orbit loss and radial electric field in DIII-D" [P5.046], Proc: 41st EPS Conf. on Plasma Physics (Berlin, Germany, 2014) http://ocs.ciemat.es/EPS2014PAP/pdf/P5.046.pdf
- [3] J.A. Boedo, E.A. Belli, E. Hollmann, W.M. Solomon, D.L. Rudakov, J.G. Watkins, R. Prater, J. Candy, R.J. Groebner, K.H. Burrell, J.S. deGrassie, C.J. Lasnier, A.W. Leonard, R.A. Moyer, G.D. Porter, N.H. Brooks, S.H. Müller, G. Tynan and E.A. Unterberg, Phys. Plasmas 18, 032510 (2011).
- [4] S.H. Müller, J.A. Boedo, K.H. Burrell, J.S. deGrassie, R.A. Moyer, D.L. Rudakov, and W.M. Solomon, Phys. Rev. Lett. **106**, 115001 (2011).
- [5] J.A. Boedo, J.S. deGrassie, B.A. Grierson, T. Stoltzfus-Dueck, D.J. Battaglia, D.L. Rudakov, E.A. Belli, R.J. Groebner, E. Hollmann, C. Lasnier, W.M. Solomon, E.A. Unterberg, J. Watkins and the DIII-D team, "Experimental Evidence of Edge Intrinsic Momentum Source Driven by Kinetic Ion Loss and Edge Radial Electric Fields in Tokamaks," submitted to Phys. Plasmas (2015).
- [6] J.S. deGrassie, R.J. Groebner, K.H. Burrell and W.M. Solomon, Nucl. Fusion 49, 085020 (2009).
- [7] J.S. deGrassie, S.H. Müller and J.A. Boedo, Nucl. Fusion **52**, 013010 (2012).
- [8] C.S. Chang and S. Ku, Phys. Plasmas **15**, 062510 (2008).
- [9] D.J. Battaglia, K.H. Burrell, C.S. Chang, S. Ku, J.S. deGrassie, and B.A. Grierson, Phys. Plasmas 21, 072508 (2014).

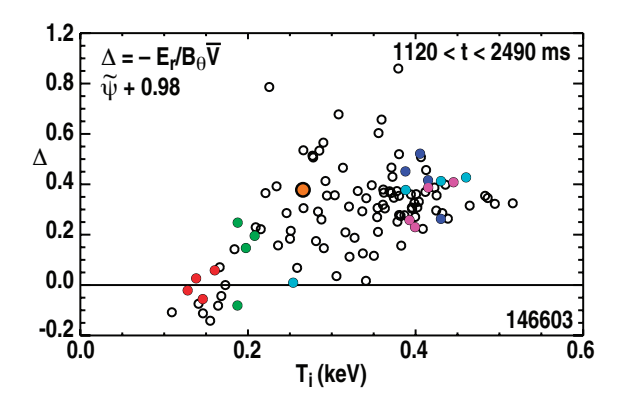
- [10] J. Seo, C. S. Chang, S. Ku, J. M. Kwon, W. Choe and S.H. Müller, Phys. Plasmas 21, 092501 (2014).
- [11] J.W. Connor and H.R. Wilson, Plasma Phys. Control Fusion **43**, R1 (2000), and references therein.
- [12] S.-I. Itoh and K. Itoh, Phys. Rev. Lett. **60**, 2276 (1988).
- [13] J. Cornelis, R. Sporken, G. van Oost and R.R. Weynants, Nucl. Fusion 34, 171 (1994).
- [14] K.C. Shaing, Phys. Fluids B 4, 3310 (1992).
- [15] L.L. Lao, H.E. St. John, Q. Peng, J.R. Ferron, E.J. Strait, T.S. Taylor, W.H. Meyer, C. Zhang, K.I. You, Fusion Sci. Technol. 48, 968 (2005).
- [16] J.A. Heikkinen, T.P. Kiviniemi and A.G. Peeters, Phys. Rev. Lett. 84, 487 (2000).
- [17] K.C. Shaing, Phys. Plasmas 9, 1 (2002).
- [18] J.S. deGrassie, R.J. Groebner and K.H. Burrell, Phys. Plasmas 13, 112507 (2006).
- [19] R.C. Isler, Plasma Phys. Control. Fusion **36**, 171 (1994).
- [20] Allen H. Boozer, Phys. Fluids 19, 149 (1976).
- [21] K.C. Shaing and E.C. Crume Jr., Phys. Rev. Lett. **63**, 2369 (1989).

- Fig. 1. (Color online) (a) time traces for averaged electron density, n_e , and NBI power, P_{NBI} . (b) ECH power, P_{ECH} , normalized beta, β_N , and $D\alpha$ recycling light.
- Fig. 2. (Color online) Δ versus $T_{\rm i}$ at $\tilde{\psi}$ = 0.98 for the discharge in Fig. 1 over the time range indicated. The colors correspond to the times indicated in Fig. 1(b).
- Fig. 3. (Color online) Contours of the $\tilde{\lambda}_1$ computed solution of eqn (3) versus Δ and $Z_{\rm eff}$ at $\tilde{\psi}$ = 0.98 at the timeslice indicated in Fig. (2). The measured values of Δ and $Z_{\rm eff}$ are indicated by the straight lines (red online). The shaded region indicates the error bars. The measured value of the $\tilde{\lambda}_1$ contour is also indicated (red online).
- Fig. 4. (Color online) Phenomenological circuit for generation of edge $E_{\rm r}$ in the "steady state" limit, $v_{\rm d}t >> 1$. $U_{\rm co}$ presents an electromotive force (EMF), and $\varepsilon_{\rm NC}$ is the neoclassical dielectric.



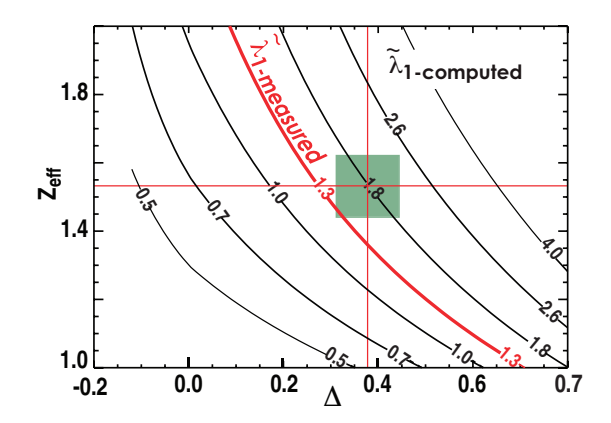
J.S. deGrassie

Fig. 1



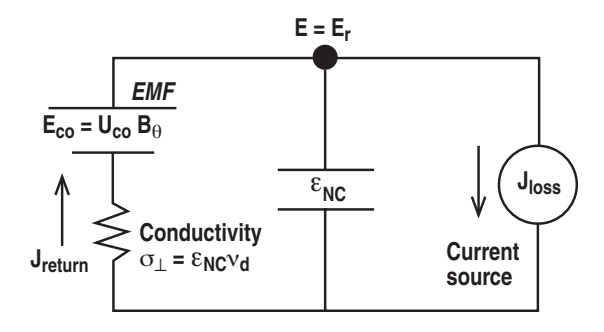
J.S. deGrassie

Fig. 2



J.S. deGrassie

Fig. 3



J.S. deGrassie

Fig. 4

